

FULL PAPER

Open Access



Five parameters for the evaluation of the soil nonlinearity during the Ms8.0 Wenchuan Earthquake using the HVSr method

Yefei Ren , Ruizhi Wen *, Xinxin Yao and Kun Ji

Abstract

The consideration of soil nonlinearity is important for the accurate estimation of the site response. To evaluate the soil nonlinearity during the 2008 Ms8.0 Wenchuan Earthquake, 33 strong-motion records obtained from the main shock and 890 records from 157 aftershocks were collected for this study. The horizontal-to-vertical spectral ratio (HVSr) method was used to calculate five parameters: the ratio of predominant frequency (RF_p), degree of nonlinearity (DNL), absolute degree of nonlinearity (ADNL), frequency of nonlinearity (fNL), and percentage of nonlinearity (PNL). The purpose of this study was to evaluate the soil nonlinearity level of 33 strong-motion stations and to investigate the characteristics, performance, and effective usage of these five parameters. Their correlations with the peak ground acceleration (PGA), peak ground velocity (PGV), average uppermost 30-m shear-wave velocity (V_{S30}), and maximum amplitude of HVSr (A_{max}) were investigated. The results showed that all five parameters correlate well with PGA and PGV. The DNL, ADNL, and PNL also show a good correlation with A_{max} , which means that the degree of soil nonlinearity not only depends on the ground-motion amplitude (e.g., PGA and PGV) but also on the site condition. The fNL correlates with PGA and PGV but shows no correlation with either A_{max} or V_{S30} , implying that the frequency width affected by the soil nonlinearity predominantly depends on the ground-motion amplitude rather than the site condition. At 16 of the 33 stations analyzed in this study, the site response showed evident (i.e., strong and medium) nonlinearity during the main shock of the Wenchuan Earthquake, where the ground-motion level was almost beyond the threshold of $PGA > 200 \text{ cm/s}^2$ or $PGV > 15 \text{ cm/s}$. The site response showed weak and no nonlinearity at the other 14 and 3 stations. These results also confirm that RF_p , DNL, ADNL, and PNL are effective in identifying the soil nonlinearity behavior. The identification results vary for different parameters because each parameter has individual features. The performance of the PNL was better than that of DNL and ADNL in this case study. The thresholds of ADNL and PNL are proposed to be 2.0 and 7%, respectively.

Keywords: Wenchuan Earthquake, Soil nonlinearity, Site response, HVSr method, DNL, PGA, PGV, V_{S30}

Introduction

It is well known that seismic waves can be amplified by surface soil layers that have a strong impedance contrast with deep bedrock. This is often called site response (or soil amplification) and can exacerbate earthquake damage such as in the 1985 Mexico Earthquake (Celebi et al. 1987) and 1989 Loma Prieta Earthquake in the USA

(Borcherdt and Glassmoyer 1992). It is therefore important to the earthquake engineering community to be able to accurately evaluate the site response. However, there has been a long-standing debate between geotechnical engineers and seismologists over whether site response is linearly or nonlinearly associated with ground-motion amplitude (Field et al. 1997; Beresnev and Wen 1996).

Real strong-motion records of the 1994 Northridge Earthquake in the USA were cited as direct evidence of nonlinear site response (e.g., Trifunac and Todorovska 1996; Beresnev et al. 1998; Hartzell 1998). When the ground motion exceeds a certain threshold, site response

*Correspondence: ruizhi@iem.ac.cn

Key Laboratory of Earthquake Engineering and Engineering Vibration, Institute of Engineering Mechanics, China Earthquake Administration, No. 29 Xuefu Road, Harbin 150080, Heilongjiang, People's Republic of China

changes occur, reflecting a shift of the resonant frequencies toward lower values and a reduction in the associated amplification. Further evidence has been observed for many subsequent strong earthquake events such as the 1995 Kobe Earthquake in Japan (Aguirre and Irikura 1997; Pavlenko and Irikura 2002), 1999 Chi-chi Earthquake in Taiwan (Pavlenko and Loh 2005; Pavlenko and Wen 2008), 2011 Christchurch Earthquake in New Zealand (Wen et al. 2011), and 2011 Tohoku Earthquake in Japan (Bonilla et al. 2011).

Many methods were proposed in previous studies to identify the nonlinearity of the site response such as the transfer function method (Wen 1994) and horizontal-to-vertical spectral ratio (HVSr) method. Because of its simplicity and ease of operation, the HVSr method has been used successfully in evaluating the nonlinear site response of several typical earthquakes, such as the 1994 Northridge Earthquake (Dimitriu 2002) and 2010 Darfield Earthquake sequence in New Zealand (Wen et al. 2011), and some observational networks such as the Kyoshin network (K-net) and Kiban Kyoshin network (KiK-net; Régnier et al. 2013, 2016).

The HVSr method has also been used to evaluate the nonlinearity of the site response of the 2008 Ms8.0 Wenchuan Earthquake. For example, using the HVSr method together with the short-term Fourier transform, Xu (2010) identified clear soil nonlinearity for sites that recorded peak ground acceleration (PGA) >200 cm/s². It was found that these sites were located in areas where soil liquefaction was observed. Rong et al. (2016) used the HVSr method to investigate the nonlinear site response at 21 strong-motion stations. They found that the predominant frequency decreased with increasing ground-motion level, but they did not observe a decrease in the amplitude of the soil amplification because of limited data. However, these studies did not systematically investigate the features of some parameters that could be used to quantitatively evaluate the level of soil nonlinearity such as the degree of nonlinearity (DNL). This parameter was defined by Noguchi and Sasatani (2008) and has been used in many case studies such as for the identification of the soil nonlinearity of strong-motion sites at the ocean bottom (Dhakal et al. 2017).

The objective of this study was to evaluate the level of soil nonlinearity of 33 strong-motion stations using five parameters and to identify the PGA and peak ground velocity (PGV) thresholds beyond which the site response evidently behaved nonlinearly during the Wenchuan main shock. These parameters include DNL, frequency of nonlinearity (fNL), and percentage of nonlinearity (PNL), defined by Régnier et al. (2013), and the ratio of the predominant frequency (RF_p) and absolute degree of nonlinearity (ADNL), as defined in this study.

The second objective of this study was to investigate the characteristics, performance, and effective usage of these five parameters to evaluate the nonlinear behavior of the site response. The correlations between these five parameters and PGA, PGV, average uppermost 30-m shear-wave velocity (V_{S30}), and maximum amplitude of HVSr (A_{max}) were investigated to analyze the effect of the site condition and ground-motion amplitude on the degree and frequency width of the soil nonlinearity.

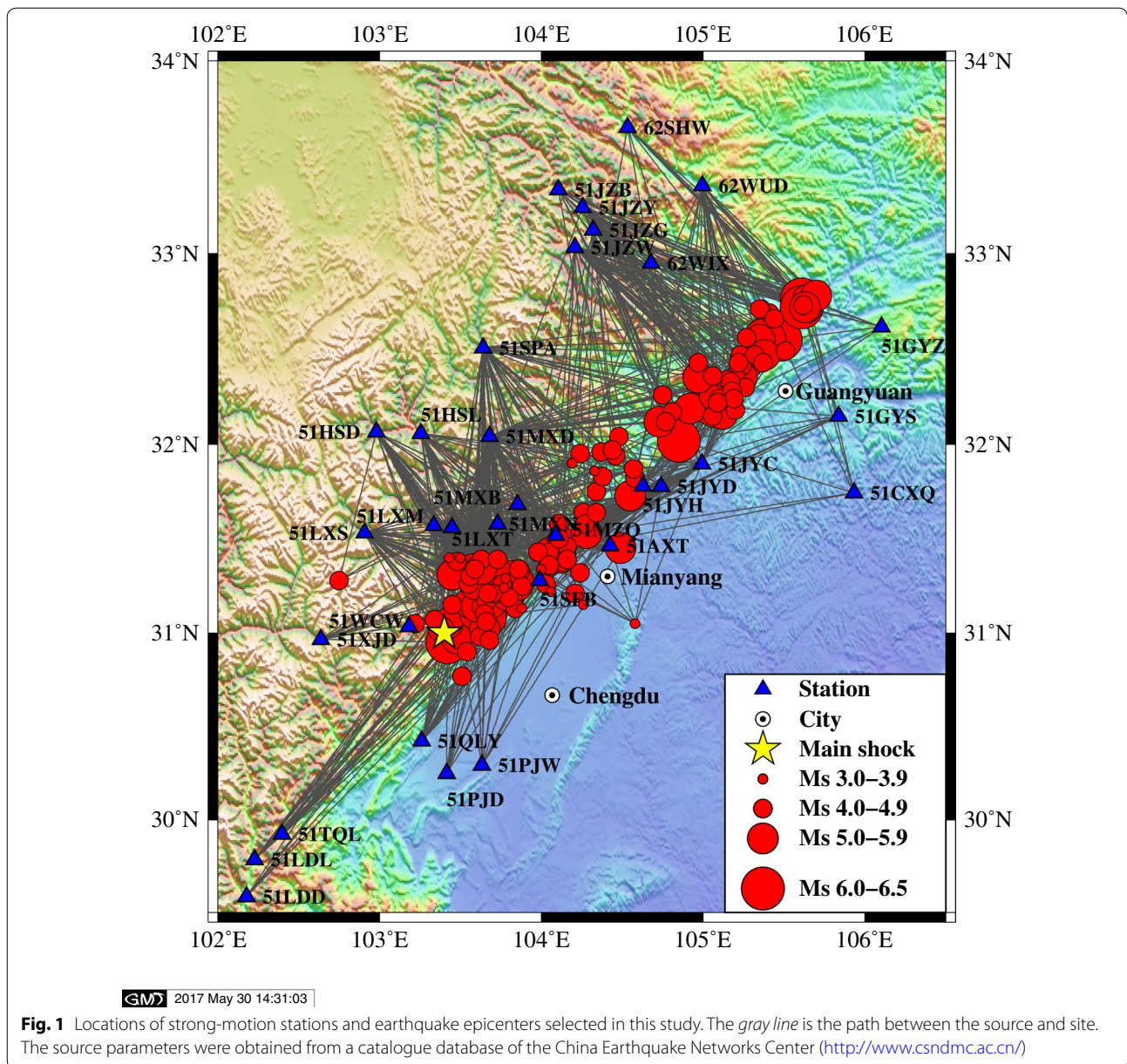
Dataset and data processing

More than 400 strong-motion records were collected during the main shock of the 2008 Ms8.0 Wenchuan Earthquake (Li et al. 2008), and more than 2000 records were acquired from 383 aftershocks (Li 2009). Several large PGAs were recorded, for example, 957.3 cm/s² at station 51WCW, -824.6 cm/s² at station 51MZQ, and -585.7 cm/s² at station 51SFB. A large ground-motion amplitude might trigger the change of the site response from the linear to nonlinear stage.

The HVSrs, representative of soil amplification, were calculated using the strong-motion records obtained from the main shock (i.e., strong motion) and aftershocks (i.e., weak motion), separately. Here, strong motion is defined as record with PGA >100 cm/s², observed in any one of the components during the main shock of the Wenchuan Earthquake. Consequently, 33 strong-motion stations were selected; their locations are shown in Fig. 1. To provide reliable estimates of PGA and PGV, a baseline correction was made to these 33 records using the method proposed by Boore (2010). The station code, PGA, PGV, and V_{S30} (proxy for the site condition) of each station are listed in Table 1.

For weak motions, the records obtained from hundreds of aftershocks were selected based on the following criteria: (1) The geometric mean of PGA of two horizontal components should be >2 and <100 cm/s². The lower boundary is assigned to avoid noise contamination and the upper boundary value is set to remove data potentially affected by soil nonlinearity. Many studies reported that the threshold of PGA causing nonlinear site response is >100 cm/s² (e.g., Régnier et al. 2016; Dhakal, et al. 2017); (2) to ensure a relatively low level of scattering of the HVSr results, each station should provide at least three records that match criterion (1).

Overall, 890 records from 157 aftershocks were available for this study. Figure 1 shows the epicenters of these aftershocks and the locations of the corresponding triggered stations. The magnitude–distance and magnitude–PGA distributions of these records are shown in Fig. 2, clearly illustrating that the records have uniform distribution within a range <200 km.



A Butterworth filter with a bandwidth of 0.3–25.0 Hz was applied to each record. The S-wave portion was then detected following the method of Ren et al. (2013). To remove truncation errors, a cosine-type tapered window was used. The Fourier amplitude spectrum (FAS) for each component was calculated. A 0.5-Hz-width Parzen window was then used to smooth the spectrum. Finally, the resultant horizontal FAS $H(f)$ was determined based on the geometric mean using Eq. (1), where $H_1(f)$ and $H_2(f)$ represent the FAS of two orthogonal horizontal components:

$$\ln H(f) = \frac{\ln H_1(f) + \ln H_2(f)}{2} \quad (1)$$

Site response calculated with the HVSR method

The site responses of the 33 stations in the frequency range of 0.5–20.0 Hz were calculated individually using the HVSR method for strong and weak motions, as shown in Figs. 3 and 4. Multiple HVSR curves produced a geometric mean, which was used to determine the site response under weak motions, while only one curve was available for strong motions. It clearly shows that site response under strong motion is considerably smaller than that under weak motion in the high-frequency band for stations 51GYS, 51GYZ, 51JYC, 51JYD, 51JYH, 51SFB, and 51WCW, and the predominant frequency (F_p) significantly shifts from high to low frequency. This

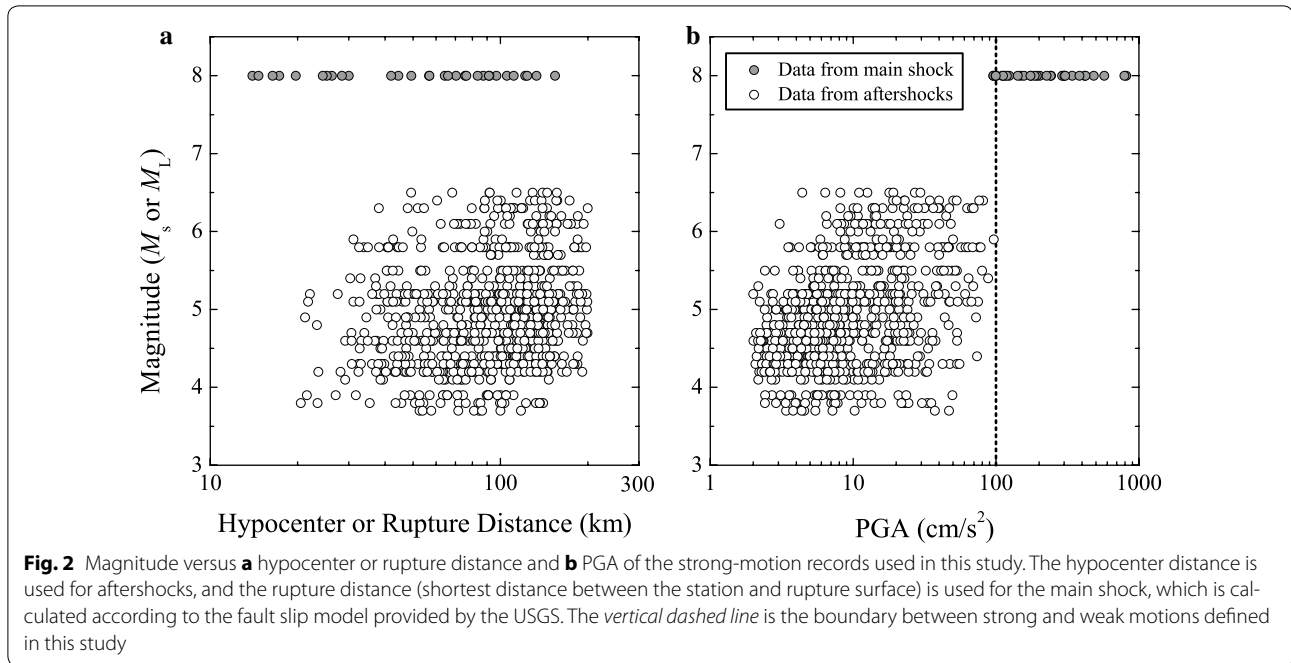
Table 1 Site conditions of the 33 strong-motion stations and the recorded PGA and PGV values during the Ms8.0 Wenchuan Earthquake and parameters identified for the evaluation of the soil nonlinearity

No.	Station code ^a	Record number	V_{330}^a (m/s)	A_{max}	PGA (cm/s ²)		PGV (cm/s)		F_p (Hz)			fNL (Hz)	DNL	ADNL	PNL (%)	Nonlinearity level		
					EW	NS	Mean	EW	NS	Mean	Weak						Strong	RF _p
1	51AXT	8	376.1	4.95	-289.4	203.4	242.6	29.0	-31.3	30.1	3.91	2.98	1.31	7.96	4.98	0.21	6.78	Medium
2	51CKQ	5	542.0	4.32	-184.8	-166.9	175.7	-22.9	14.2	18.0	3.96	3.56	1.11	10.21	2.48	0.08	1.87	Weak
3	51GVS	10	388.2	11.01	320.4	274.0	296.3	-20.5	23.7	22.0	8.25	4.79	1.72	6.69	5.38	0.37	24.13	Strong
4	51GVZ	6	366.5	6.50	424.4	-410.6	417.5	27.5	-42.0	34.0	4.20	2.15	1.95	2.83	4.07	0.37	26.81	Strong
5	51HSD	31	366.6	5.14	-102.5	89.8	95.9	6.2	5.3	5.7	12.21	11.08	1.10	11.52	2.77	0.09	5.82	Weak
6	51HSL	33	351.3	3.31	-107.6	-142.6	123.9	7.4	9.4	8.3	3.56	3.61	0.99	11.57	2.73	0.08	3.15	Weak
7	51JYC	60	430.5	9.45	298.0	282.9	290.3	22.4	-34.2	27.7	7.28	5.42	1.34	2.88	10.55	0.75	30.52	Strong
8	51JYD	37	475.6	11.64	-510.1	456.8	482.7	27.3	34.4	30.6	8.01	3.71	2.16	6.64	6.52	0.41	20.79	Strong
9	51JYH	33	322.8	5.58	-512.9	-347.7	422.3	20.6	-30.0	24.8	12.89	7.67	1.68	8.30	5.93	0.27	12.06	Strong
10	51JZB	13	354.3	3.90	-96.4	104.6	100.4	-4.7	-4.1	4.4	2.93	2.83	1.03	12.55	2.90	0.13	7.50	Medium
11	51JZG	34	325.6	3.19	-169.8	241.4	202.5	-10.9	8.6	9.7	5.18	4.83	1.07	8.01	2.64	0.09	2.87	Weak
12	51JZW	40	457.3	4.88	-128.1	173.6	149.2	-9.8	10.0	9.9	4.44	3.42	1.30	8.20	4.13	0.17	8.88	Medium
13	51JZY	31	340.6	3.80	-91.7	100.0	95.8	-7.8	-7.3	7.5	6.74	6.25	1.08	6.49	2.49	0.07	2.27	Weak
14	51LDD	5	378.0	6.96	109.3	-111.8	110.5	6.2	-7.6	6.9	1.86	1.61	1.15	9.33	3.02	0.17	3.41	Weak
15	51LDL	11	348.6	6.84	-109.3	-120.5	114.7	4.9	6.4	5.6	2.34	2.44	0.96	8.69	3.16	0.16	5.52	Weak
16	51LXM	73	325.5	8.76	320.9	-283.8	301.8	22.4	19.0	20.6	2.73	2.44	1.12	7.23	3.14	0.13	6.64	Weak
17	51LXS	43	340.9	3.20	221.3	261.7	240.7	9.1	8.8	8.9	3.81	3.66	1.04	11.77	3.33	0.16	6.38	Weak
18	51LXT	70	350.8	2.27	339.6	342.2	340.9	19.1	13.0	15.7	7.18	6.69	1.07	6.10	4.42	0.17	5.20	Medium
19	51MXT	13	584.6	2.08	-306.6	302.2	304.4	27.7	-20.4	23.7	-	-	-	2.07	0.07	4.09	None	
20	51MXD	87	299.4	4.26	246.6	-206.1	225.5	-17.5	-33.4	24.2	0.98	0.98	1.00	5.08	2.61	0.12	3.24	Weak
21	51MXN	65	430.0	3.53	-421.1	349.2	383.5	33.3	26.9	29.9	1.61	1.51	1.06	5.81	3.86	0.18	7.76	Medium
22	51MZQ	3	551.3	3.52	-824.6	803.3	813.9	-136.3	66.3	95.0	4.59	3.76	1.22	3.96	4.19	0.32	16.96	Medium
23	51PID	9	389.5	8.24	-195.8	-190.3	193.0	19.6	-15.5	17.4	2.78	2.69	1.04	11.67	2.78	0.16	4.31	Weak
24	51PIW	11	337.9	5.62	97.7	101.2	99.4	-20.0	10.1	14.2	3.61	3.42	1.06	8.79	3.09	0.15	5.64	Weak
25	51QLY	19	508.5	7.62	-173.7	-199.8	186.3	16.5	8.3	11.7	6.74	6.20	1.09	9.67	3.02	0.13	6.14	Weak
26	51SFB	8	379.3	12.34	558.2	-585.7	571.8	-85.0	79.1	82.0	6.98	2.73	2.55	4.10	9.58	0.99	48.53	Strong
27	51SPA	56	374.4	3.82	-186.6	131.6	156.7	-6.9	-8.0	7.5	6.59	6.01	1.10	10.60	2.30	0.08	2.82	Weak
28	51TQL	8	526.3	7.86	-122.1	116.2	119.1	3.5	-3.4	3.5	8.30	7.67	1.08	7.76	3.13	0.16	10.76	Medium
29	51WCW	9	511.2	7.81	957.3	652.4	790.3	-53.4	45.0	49.1	8.74	2.15	4.07	4.54	10.50	1.01	44.78	Strong
30	51XD	9	370.2	2.45	-94.9	132.1	112.0	-5.9	-9.9	7.7	5.32	3.66	1.45	-	1.63	0.05	2.85	Medium
31	62SHW	9	419.0	2.80	-91.4	108.8	99.7	-9.2	6.1	7.5	4.59	5.81	0.79	-	2.58	0.09	3.79	None
32	62WX	9	584.6	1.50	-142.6	-141.1	141.9	11.8	9.1	10.4	-	-	-	-	0.94	0.00	0.22	None
33	62WUD	32	227.8	5.50	-184.8	-163.9	174.1	-16.5	13.5	14.9	1.07	1.12	0.96	4.69	5.00	0.30	8.94	Medium

"-" means that F_p and fNL cannot be identified

^a The V_{330} data were taken from the NGA-West2 database (<http://peer.berkeley.edu/ngawest2/databases/>)

^b Stations 51MXT and 62WX are located at rock sites, and the other stations are located at alluvial sites based on station construction reports



implies that strong soil nonlinearity occurred during the main shock at these stations. Although less evident, a similar phenomenon can be observed at stations 51AXT, 51JZW, 51LXS, 51QLY, 51TQL, and 62WUD, implying medium or weak nonlinearity.

The values of PGA and PGV, recorded during the main shock, and V_{S30} for each station are also presented in Figs. 3 and 4. It can be observed that the sites at which a small PGA or PGV was recorded, such as 51HSD, 51HSL, 51LDD, 51LDL, 51XJD, and 62SHW, show weak evidence of soil nonlinearity. Furthermore, there is absolutely no evidence of soil nonlinearity for sites without covering soil such as 51MXT and 62WIX. According to station construction reports, only 51MXT and 62WIX are located at rock sites. The other stations are located at alluvial sites. Therefore, the correlations of the nonlinearity with PGA, PGV, V_{S30} , and A_{\max} should be analyzed in detail considering the purpose of this study.

Definition of the five parameters used to evaluate the soil nonlinearity

To investigate the effects of the nonlinear behavior of soils on the site response, Régnier et al. (2013) proposed using two parameters per event and four parameters per site based on various earthquake records from the KiK-net database in Japan. The fNL and PNL were proposed by their study, the DNL was proposed by Noguchi and Sasatani (2008), and RF_p and ADNL are proposed in this study.

The parameter DNL is defined as follows:

$$DNL = \sum_{i=N_1}^{N_2} \left| \log \left[\frac{R_{\text{strong}}(i)}{R_{\text{weak}}(i)} \right] \right| (f_{i+1} - f_i), \quad (2)$$

where $R_{\text{strong}}(i)$ and $R_{\text{weak}}(i)$ represent the HVSR values at the frequency f_i for S-waves during strong (PGA > 100 cm/s² in this study) and weak motions (PGA < 100 cm/s² in this study), respectively, and N_1 and N_2 represent the beginning and ending frequencies, usually set as 0.5 and 20.0 Hz. Figure 5a shows an illustration of the calculation of DNL, which actually represents the non-overlapping parts of both areas enclosing the HVSRs for S-waves during strong and weak motions and the horizontal ordinate of the frequency.

It should be noted that the average HVSR for S-waves during weak motion is used when calculating the value of DNL; however, its standard deviation is not included. To consider the effect of the standard deviation, we propose an improved parameter called the absolute degree of nonlinearity (ADNL), which is defined as follows:

$$ADNL = \sum_{i=N_1}^{N_2} \Delta(i) \cdot [\log(f_{i+1}) - \log(f_i)] \quad (3)$$

$$\Delta(i) = \begin{cases} \log(R_{\text{strong}}(i)) - \log(R_{\text{weak}}^+(i)) & R_{\text{strong}}(i) \geq R_{\text{weak}}^+(i) \\ \log(R_{\text{weak}}^-(i)) - \log(R_{\text{strong}}(i)) & R_{\text{strong}}(i) \leq R_{\text{weak}}^-(i) \\ 0 & \text{others} \end{cases}, \quad (4)$$

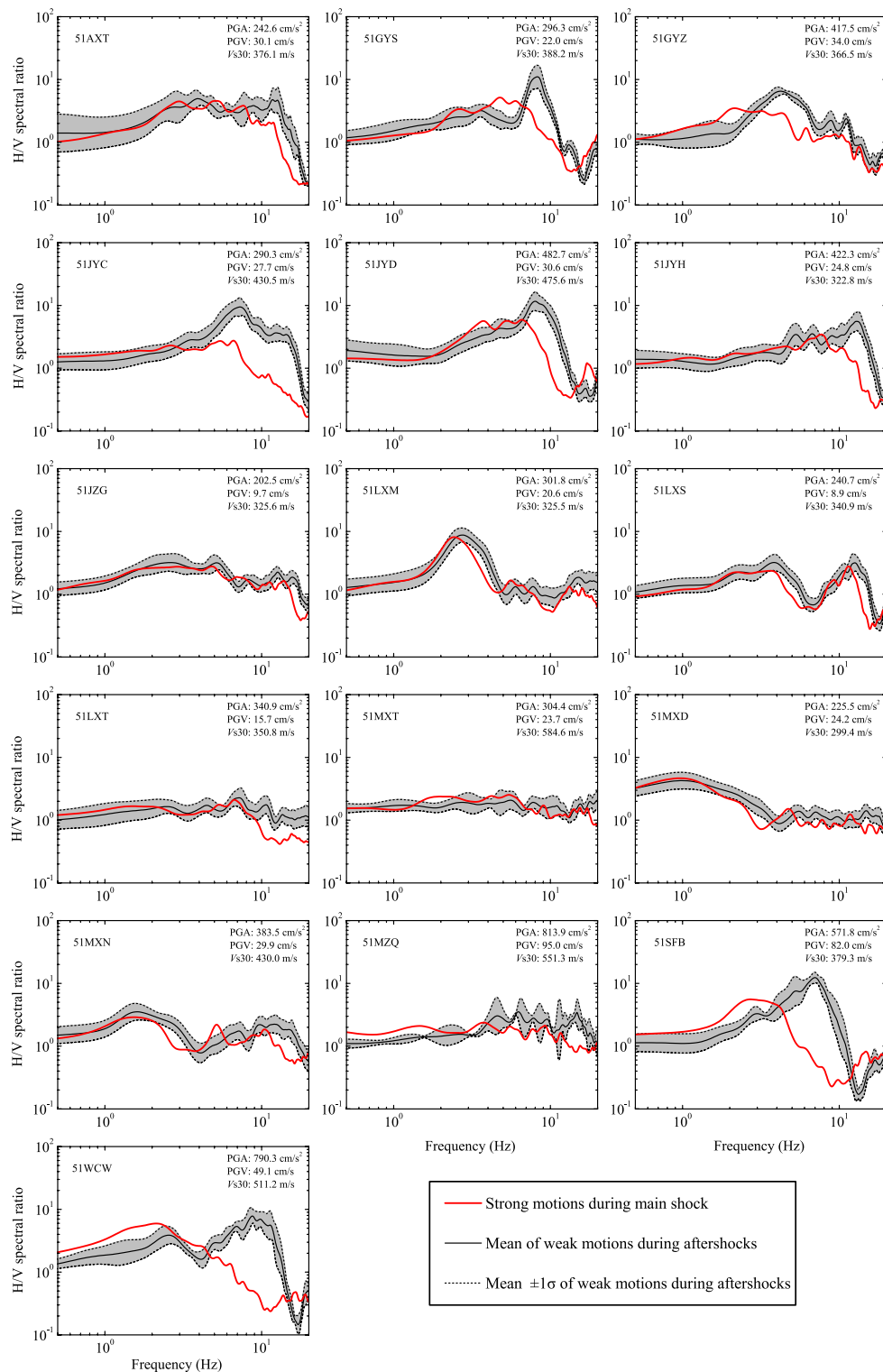


Fig. 3 Site responses calculated using the HVSR method for 16 strong-motion stations with PGA > 200 cm/s² under strong and weak motion during the 2008 Ms8.0 Wenchuan Earthquake. The V_{S30} , PGA, and PGV values recorded during the main shock for each station are presented. The shaded area indicates the range of the mean plus-minus one standard deviation

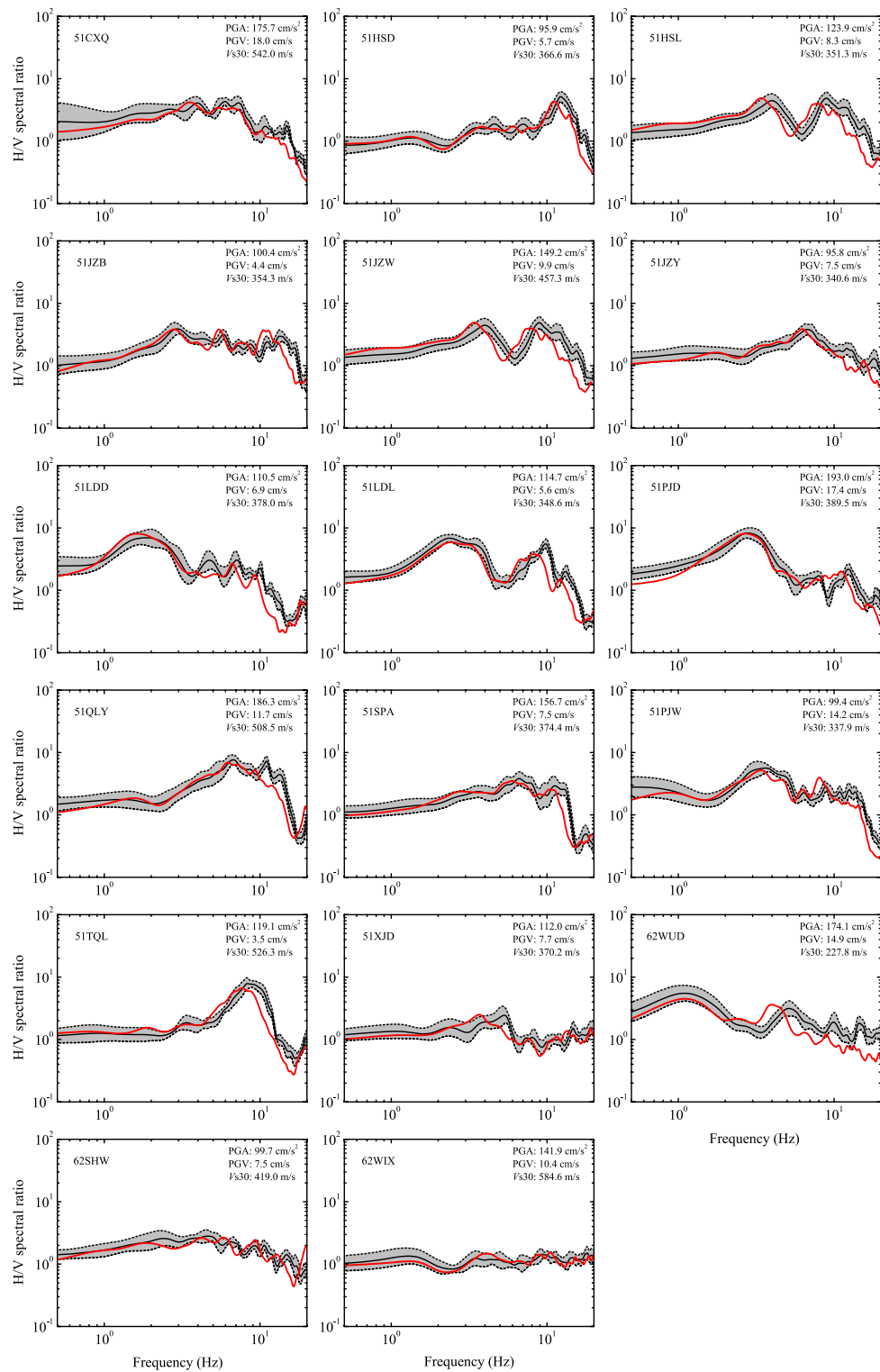


Fig. 4 Same as Fig. 3 but for 17 stations with PGA < 200 cm/s²

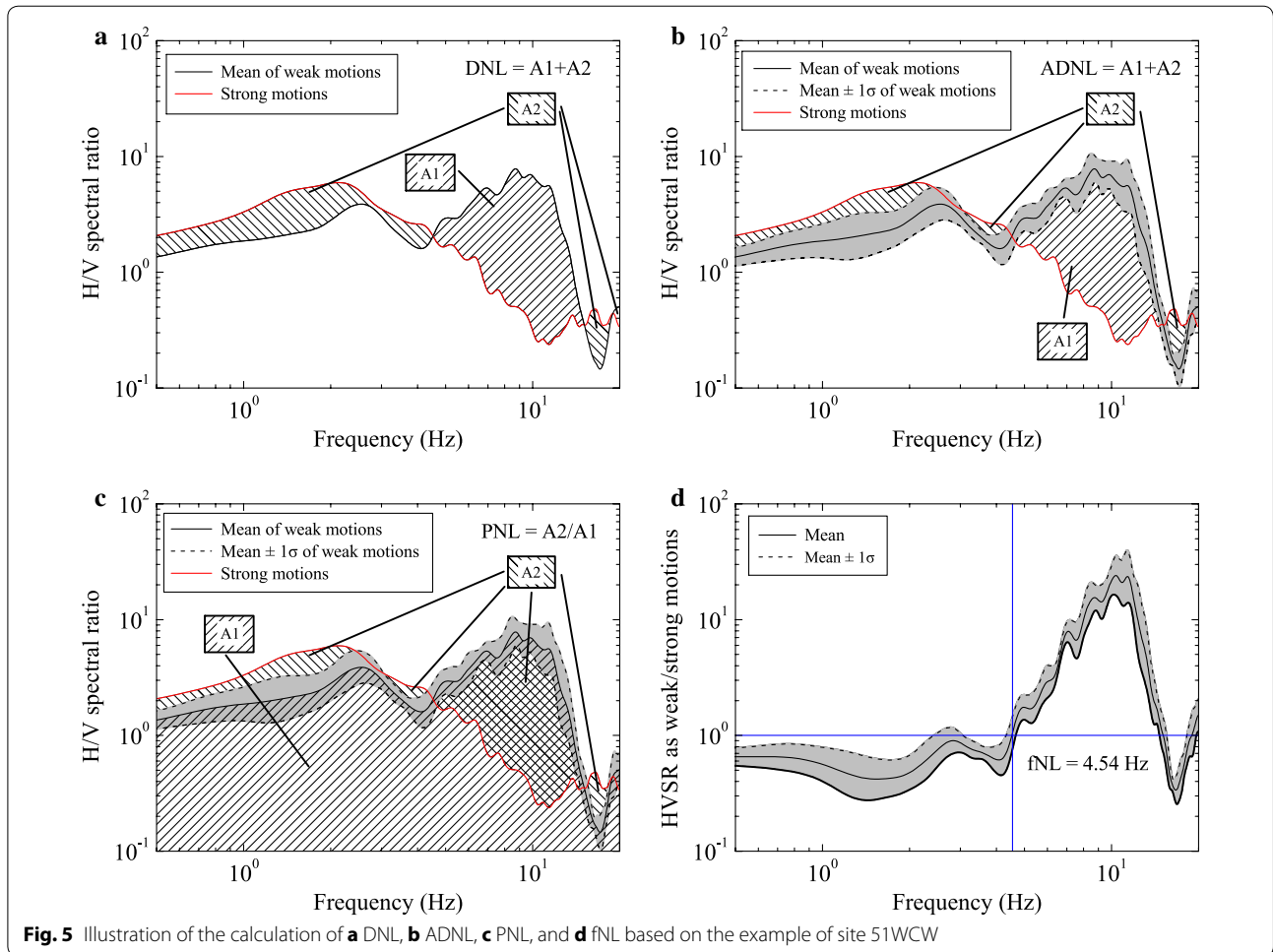


Fig. 5 Illustration of the calculation of **a** DNL, **b** ADNL, **c** PNL, and **d** fNL based on the example of site 51WCW

where $R_{\text{weak}}^+(i)$ and $R_{\text{weak}}^-(i)$ represent the values of the average HVSR plus-minus one standard deviation at the frequency f_i for S-waves during weak motion. To balance the contributions from high and low frequencies, the frequency interval was calculated on a logarithmic scale. An illustration of the calculation of ADNL is shown in Fig. 5b based on the example of site 51WCW.

The definition of PNL proposed by Régnier et al. (2013) is as follows:

$$\text{PNL} = A_2/A_1 \tag{5}$$

$$A_1 = \sum_{i=N_1}^{N_2} R_{\text{weak}}(i) \cdot [\log(f_{i+1}) - \log(f_i)] \tag{6}$$

$$A_2 = \sum_{i=N_1}^{N_2} \delta(i) \cdot [\log(f_{i+1}) - \log(f_i)] \tag{7}$$

$$\delta(i) = \begin{cases} R_{\text{strong}}(i) - R_{\text{weak}}^+(i) & R_{\text{strong}}(i) \geq R_{\text{weak}}^+(i) \\ R_{\text{weak}}^-(i) - R_{\text{strong}}(i) & R_{\text{strong}}(i) \leq R_{\text{weak}}^-(i) \\ 0 & \text{others} \end{cases} \tag{8}$$

An illustration of how to calculate PNL is shown in Fig. 5c for the example of station 51WCW, where A_1 is the area enclosing the HVSR curve derived from weak motion and the horizontal ordinate of the frequency, A_2 is the area difference between the two HVSR curves derived from weak and strong motions, and PNL represents the percentage of the relative change from linear to nonlinear site response.

Based on the definitions of DNL, ADNL, and PNL, all parameters characterize one feature of soil nonlinearity, that is, the reduction in the site response amplitude at high frequency. In fact, the frequency dependence of the effects of soil nonlinearity has been underlined in previous studies (e.g., Wen et al. 1994; Delépine et al. 2009). Régnier et al. (2013) defined the parameter fNL to reveal another feature of soil nonlinearity, that is,

the shift of the predominant frequency toward lower values.

Figure 5d shows an illustration of the calculation of fNL based on the example of site 51WCW. Taking a ratio of the HVSR of the S-wave during weak motion over that during strong motion, amplification of the nonlinear response can be observed below a given frequency compared with the linear case and deamplification takes place above this given frequency. This critical frequency is determined as the value of fNL. Notably, if fNL is smaller, it is probable that the frequency band affected by soil nonlinearity will be wider.

To clearly reveal the shift degree of the predominant frequency from linear to nonlinear site response, we defined a new parameter, RF_p , which is the ratio of the predominant frequency (F_p) under weak and strong motions:

$$RF_p = F_{p, \text{weak}} / F_{p, \text{strong}} \quad (9)$$

where $F_{p, \text{weak}}$ and $F_{p, \text{strong}}$ represent the predominant frequencies identified by HVSR curves calculated using weak and strong motions, respectively.

Evidence of soil nonlinearity during the Wenchuan main shock

The values of RF_p , DNL, ADNL, fNL, and PNL for each site were calculated (Table 1). Based on these parameters, sites showing nonlinear behavior were identified; the correlations between these parameters and PGA, PGV, V_{S30} and A_{max} were investigated.

Parameter RF_p

Figure 6 shows the parameter RF_p plotted versus the mean PGA and PGV of the two horizontal components. Note that for $PGA > 200 \text{ cm/s}^2$ or $PGV > 20 \text{ cm/s}$, F_p under strong motion becomes much smaller than under weak

motion at most sites, representative of soil nonlinearity. This phenomenon was identified at sites 51MZQ, 51WCW, 51SFB, 51JYD, 51GYZ, 51JYH, 51GYS, 51JYC, 51AXT, 51JZW, and 51XJD. The threshold of PGA used here is the same as that reported by Xu (2010) who evaluated the soil nonlinearity during the Wenchuan Earthquake using the time–frequency analysis technique. Considering the shaded area of Fig. 6, it is evident that the level of nonlinearity increases as the PGA value increases, implying strong dependence on the ground-motion amplitude.

It should be noted that the site response at station 51MZQ does not indicate soil nonlinearity behavior as strongly as station 51WCW, even though the PGA is $>800 \text{ cm/s}^2$ and the value of PGV is close to 100 cm/s . The surface geology at station 51MZQ shows only a 1.5-m-thick overburden above the soft bedrock (shear velocity $\sim 400 \text{ m/s}$), indicative of low possibility of soil nonlinearity (Ren et al. 2013). This indicates that the soil nonlinearity might be correlated with the site condition.

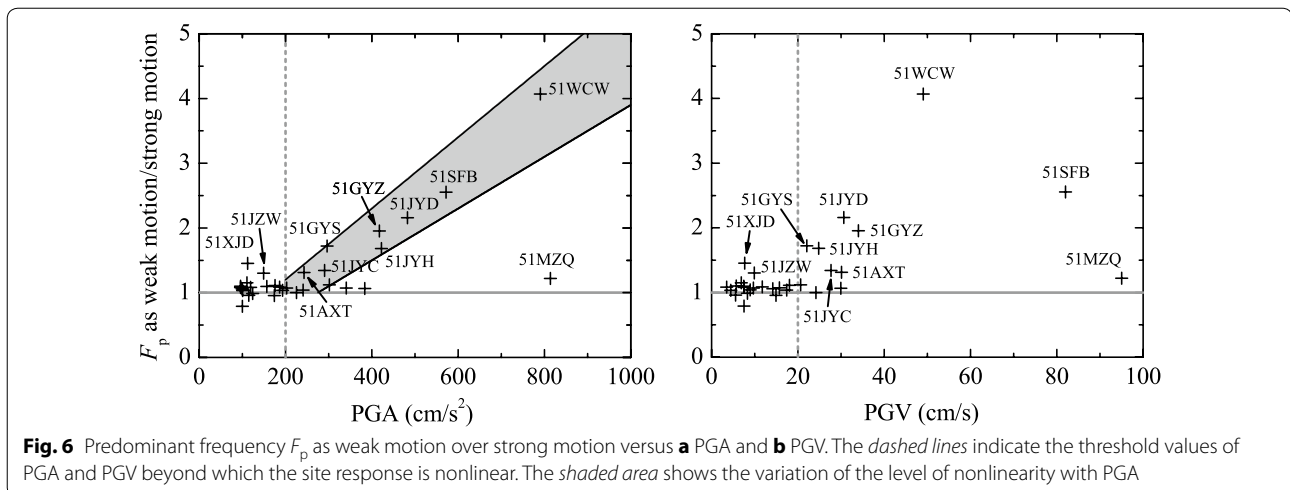
We compared the values of RF_p of this study with those provided by Ren et al. (2013) who used the generalized inversion technique. As shown in Fig. 7, the values produced by the two methods are similar for most stations, implying that our results are reliable and that our approach for the identification of the soil nonlinearity is acceptable.

Parameter DNL

The linear relationships between DNL and PGA and PGV were regressed, respectively, as shown in Fig. 8a:

$$DNL = 5.550 \cdot \log(PGA) - 8.916 \quad (R = 0.65) \quad (10)$$

$$DNL = 4.115 \cdot \log(PGV) - 0.840 \quad (R = 0.61) \quad (11)$$



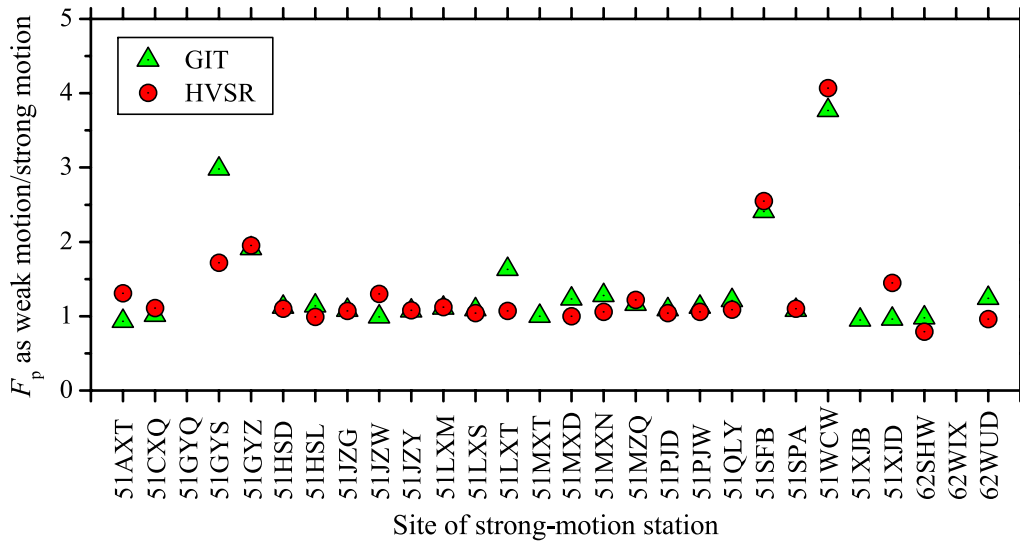


Fig. 7 Comparison of F_p as weak motion over strong motion based on the HVSR method in this study and the generalized inversion technique of Ren et al. (2013)

Because the values of DNL were calculated using the logarithmic expression of HVSR (see Eq. 2), the regressions used DNL values on a linear scale but PGA and PGV values on a logarithmic scale. In the following regressions, linear scale was also used for ADNL and PNL but logarithmic scale used for PGA, PGV, and A_{\max} . It shows that DNL positively correlates with PGA and PGV. The regression correlation coefficients of 0.65 and 0.61 indicate a moderate correlation. This is in accordance with conclusions reached in previous studies (e.g., Wen et al. 2011; Dhakal et al. 2017).

Noguchi and Sasatani (2011) suggested a DNL value of 4.0 to identify the nonlinear site response, which has been used in several previous studies such as Dhakal et al. (2017). Based on this DNL value, it could be assessed that 12 stations exhibited soil nonlinearity (Fig. 8a): 51MZQ, 51WCW, 51SFB, 51JYD, 51JYC, 51JYH, 51GYZ, 51GYS, 51LXT, 51AXT, 51JZW, and 62WUD. Most of these can also be identified using parameter RF_p .

To understand the dependence of soil nonlinearity on the site condition, we investigated the correlation between DNL and V_{S30} , as shown in Fig. 9a. The values of V_{S30} were derived from the NGA-West2 database (Ancheta et al. 2013). To eliminate the effect of the ground-motion amplitude as much as possible, the data were separated into three groups based on different PGA levels: $PGA < 200 \text{ cm/s}^2$, $200 < PGA < 400 \text{ cm/s}^2$, and $PGA > 400 \text{ cm/s}^2$. However, whichever group was used, a poor relationship between DNL and V_{S30} was observed. The values of V_{S30} in the NGA-West2 database for sites in southwest China were estimated using an extrapolation procedure based on soil

profiles at depths shallower than 30 m. It was confirmed that the values were overestimated for sites with low shear-wave velocity and underestimated for sites with high shear-wave velocity (Ancheta et al. 2013). This estimation bias might be the cause of unreliable results of the analysis of the correlation between DNL and V_{S30} .

As an alternative to V_{S30} , we used A_{\max} calculated using weak motion because A_{\max} can be considered as a proxy for the site condition. It is known that greater soil amplification can be generated at sites with a stronger impedance contrast between the surface soil layers and bedrock. Generally, large values of A_{\max} are achieved at sites with soft soil and small values of A_{\max} are obtained at sites with rigid soil or outcrops. The values of DNL versus A_{\max} are presented in Fig. 9b. An empirical relationship between them was regressed by linear fitting for each group of data. The results are as follows: when $PGA > 400 \text{ cm/s}^2$

$$DNL = 8.337 \cdot \log(A_{\max}) - 0.364 \quad (R = 0.63) \quad (12)$$

when $200 < PGA < 400 \text{ cm/s}^2$

$$DNL = 5.554 \cdot \log(A_{\max}) + 0.679 \quad (R = 0.59) \quad (13)$$

when $PGA < 200 \text{ cm/s}^2$

$$DNL = 2.803 \cdot \log(A_{\max}) + 0.988 \quad (R = 0.64) \quad (14)$$

The respective correlation coefficient (R) of 0.63, 0.59, and 0.64 for each regression indicates a moderate correlation between DNL and A_{\max} . This implies that the degree of soil nonlinearity significantly depends on the site condition.

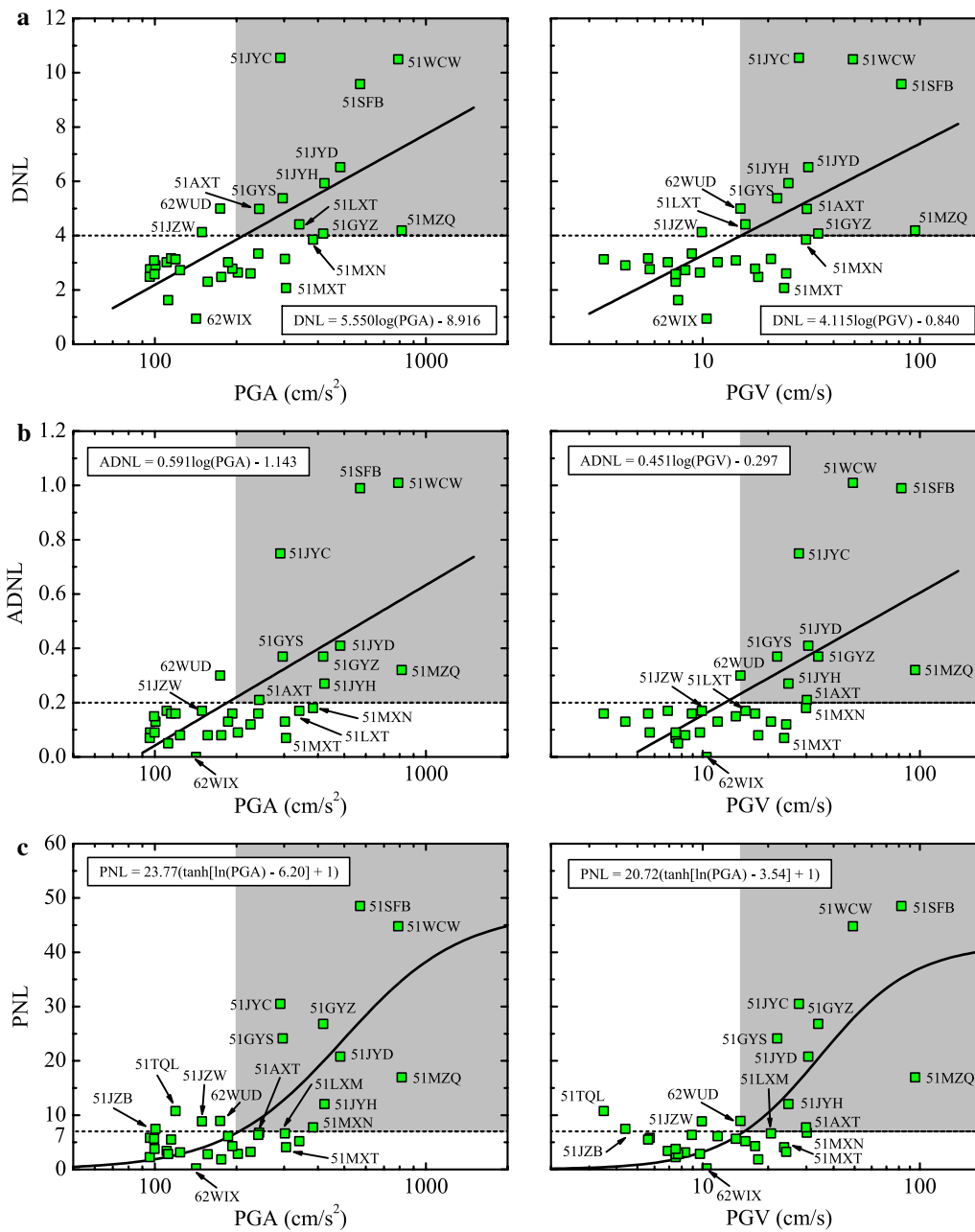


Fig. 8 Values of **a** DNL, **b** ADNL, and **c** PNL for the 33 stations versus the recorded PGAs and PGVs during the Wenchuan Earthquake including empirical relationship fitting. The *dashed lines* indicate the threshold of DNL, ADNL, and PNL proposed in this study (i.e., 4.0, 0.2, and 7%) beyond which the site response exhibits evident nonlinear behavior. The *shaded areas* indicate the regions covering the values of DNL (or ADNL, PNL) and PGA (or PGV) beyond their thresholds. The PGA and PGV thresholds are proposed to be 200 cm/s² and 15 cm/s, respectively

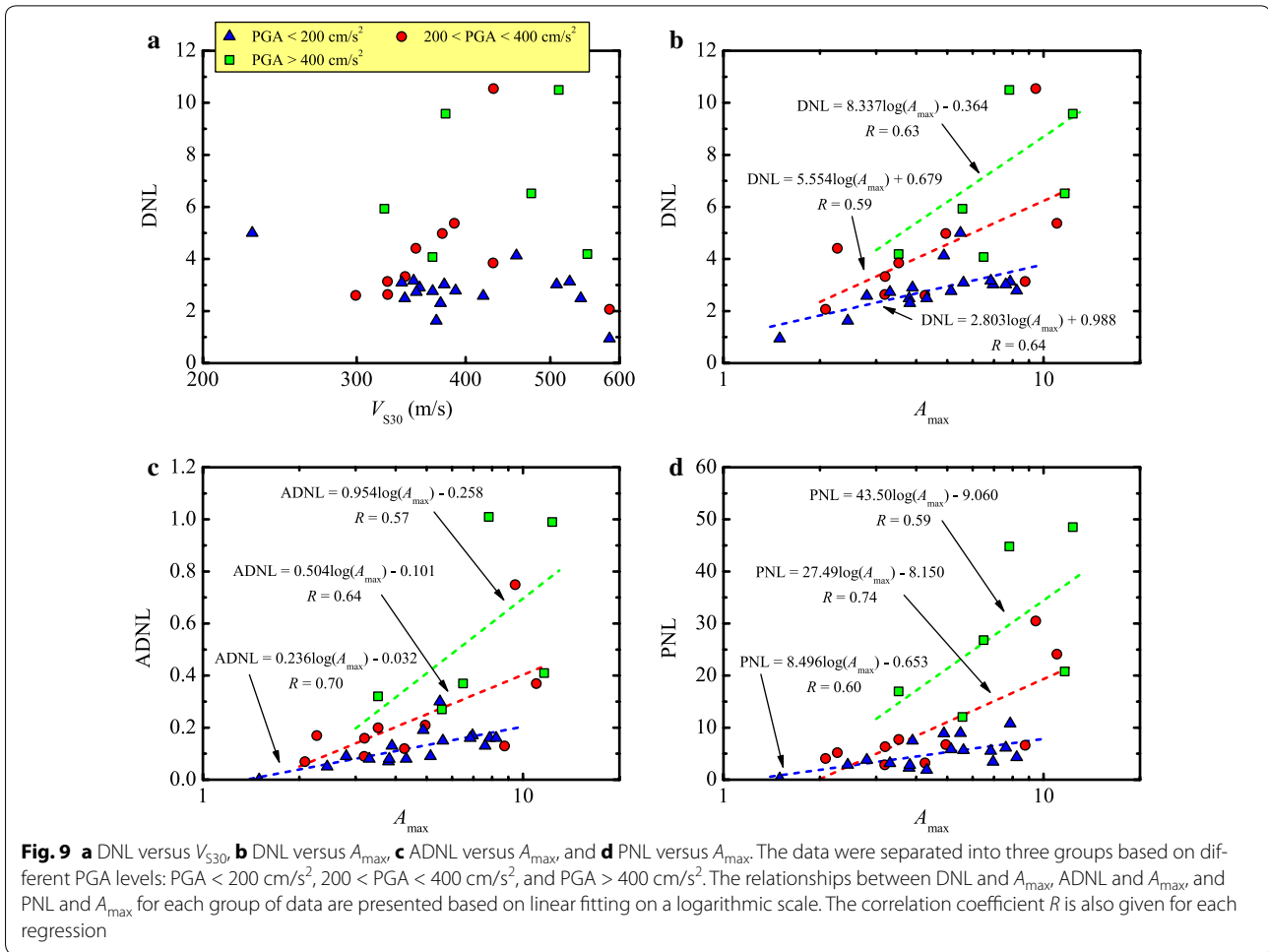
Parameter ADNL

The empirical linear relationships between ADNL and PGA and PGV were also regressed (Fig. 8b):

$$ADNL = 0.591 \cdot \log(PGA) - 1.143 \quad (R = 0.66) \quad (15)$$

$$ADNL = 0.451 \cdot \log(PGV) - 0.297 \quad (R = 0.65) \quad (16)$$

The *R* value is 0.66 and 0.65, respectively, indicating moderate correlations, similar to the relationships between DNL and PGA and PGV. The empirical relationships between ADNL and *A*_{max} were also regressed (Fig. 9c), implying moderate correlation.



Parameter fNL

Table 1 shows the value of fNL for each site. Note that fNL could not be identified at four sites (51MXT, 51XJD, 62SHW, and 62WIX) because of the small difference of the HVSR during strong and weak motions, implying the absence of soil nonlinearity.

The dependence of fNL on PGA and PGV was investigated, as shown in Fig. 10a, b. To eliminate the effect of the site condition as much as possible, the data were separated into two groups based on different A_{max} levels: $A_{\text{max}} < 5.0$ and $A_{\text{max}} > 5.0$. The reason behind using A_{max} rather than V_{S30} was already explained for the analysis of DNL. The empirical relationships between fNL and PGA and PGV were regressed for each group of data:

when $A_{\text{max}} > 5.0$

$$\log(\text{fNL}) = -0.405 \cdot \log(\text{PGA}) + 1.781 \quad (R = 0.61) \quad (17)$$

$$\log(\text{fNL}) = -0.336 \cdot \log(\text{PGV}) + 1.234 \quad (R = 0.64) \quad (18)$$

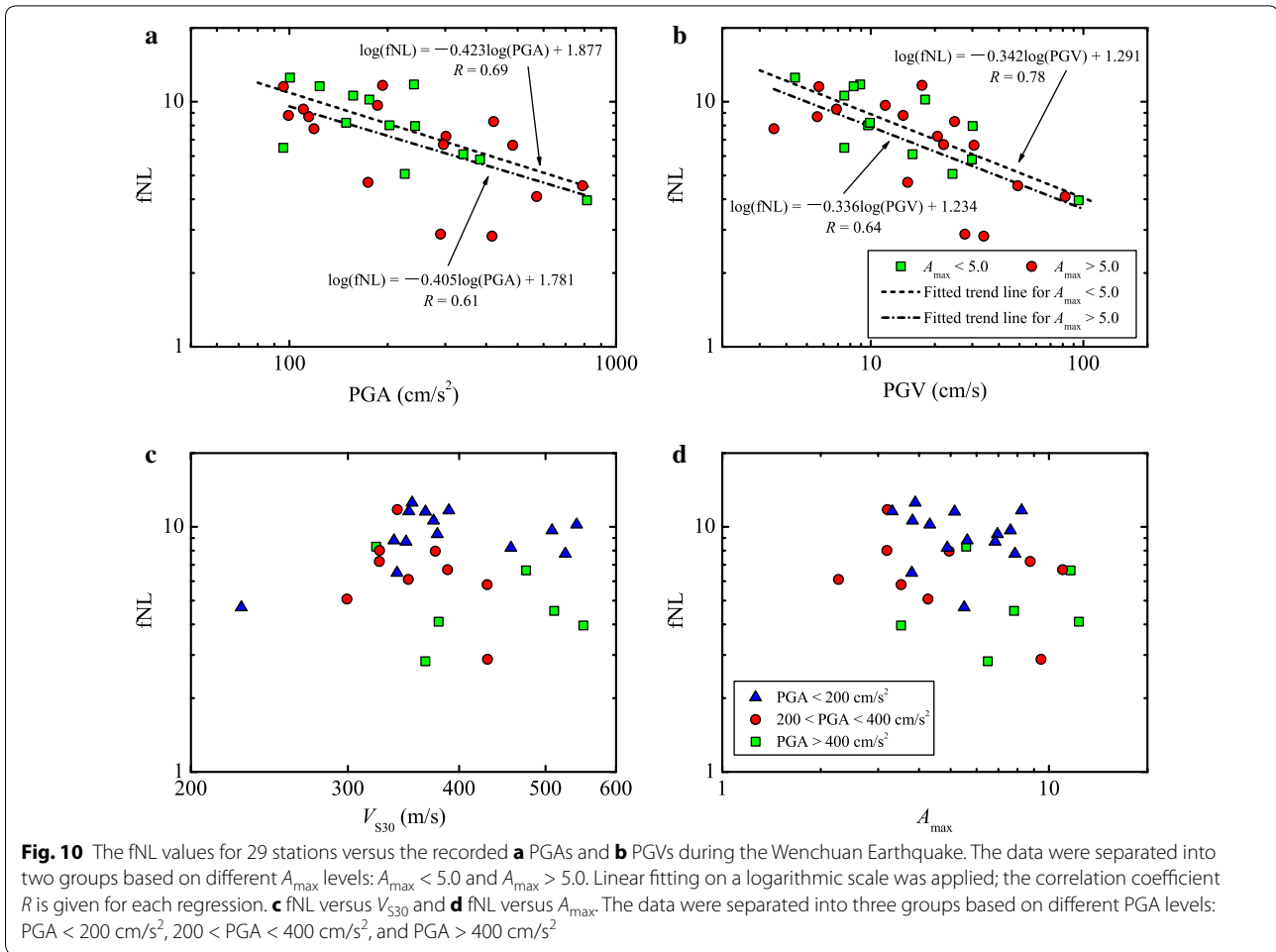
when $A_{\text{max}} < 5.0$

$$\log(\text{fNL}) = -0.423 \cdot \log(\text{PGA}) + 1.877 \quad (R = 0.69) \quad (19)$$

$$\log(\text{fNL}) = -0.342 \cdot \log(\text{PGV}) + 1.291 \quad (R = 0.78) \quad (20)$$

The respective value of R is larger than 0.6 for each regression, showing moderate correlations between fNL and PGA and PGV. The value of fNL decreases as PGA increases, consistent with the above-mentioned observation that RF_p depends on PGA. The value of RF_p increases as PGA increases, which means that the predominant frequency shifts toward the low-frequency band, which could cause a wider frequency band affected by soil nonlinearity and consequently a lower fNL value.

The dependences of fNL on V_{S30} and A_{max} were investigated, as shown in Fig. 10c, d, respectively. The data were also separated into three groups based on different PGA levels. The figures show that there is no correlation



between fNL and V_{S30} or A_{\max} , whichever group of data was analyzed. This is in accordance with the conclusion by Régnier et al. (2013) who determined a regression correlation coefficient of only 0.35 between fNL and V_{S30} . Therefore, the frequency width affected by soil nonlinearity predominantly depends on the ground-motion amplitude (e.g., PGA or PGV) rather than the site condition.

Parameter PNL

Figure 8c shows the correlations between PNL and PGA and PGV. The empirical relationships between these parameters were regressed using the following equation (Régnier et al. 2013):

$$\text{PNL} = a \cdot \{ \tanh[\ln(\text{PGA}) - b] + 1 \}, \quad (21)$$

where a and b are the regression coefficients, that is, $a = 23.77$ and $b = 6.20$ for PGA and $a = 20.72$ and $b = 3.54$ for PGV, obtained in this study. The correlation coefficient is 0.73 for both PGA and PGV, revealing that PNL has a strong positive correlation with PGA or PGV, similar to the other parameters (RF_p , DNL, and ADNL).

The empirical relationship between PNL and A_{\max} was also regressed (Fig. 9d), indicating that PNL has a moderate positive correlation with A_{\max} , similar to DNL and ADNL.

Discussion

Our analysis shows that all five parameters have moderate correlations with PGA or PGV, proving the dependence of the soil nonlinearity on the ground-motion amplitude. The larger the ground motion is, the stronger the soil nonlinearity is. In addition, the soil nonlinearity also depends on the site condition; Fig. 9 shows that DNL, ADNL, and PNL positively correlate with A_{\max} . A larger A_{\max} value generally corresponds to a stronger impedance contrast between the surface soil layers and overburden bedrock; therefore, the softer the soil layer is, the stronger the soil nonlinearity is. Note that stations 51MXT and 62WIX are located at rock sites, leading to small values of DNL, ADNL, and PNL, as shown in Fig. 8. Although the PGAs reached to 304.4 and 141.9 cm/s^2 , respectively, there is no evidence of soil nonlinearity at both stations.

The distribution of RF_p versus PGA shown in Fig. 6 represents a PGA threshold of 200 cm/s^2 beyond which most stations evidently show nonlinear site response. The same PGA threshold was also derived from the regressed relationships between DNL and PGA shown in Fig. 8a based on a DNL threshold of 4.0 suggested by Noguchi and Sasatani (2011). Based on Fig. 4, the site responses under strong and weak motions do not differ much for most stations at which the recorded PGAs are almost below 200 cm/s^2 during the Wenchuan main shock.

Corresponding to the threshold of PGA (i.e., 200 cm/s^2), the threshold of ADNL was proposed to be 0.2. Beyond this value, 10 stations exhibited evident soil nonlinearity. Two sites (51JZW and 51LXT) that were included when using the DNL parameter (see Fig. 8a, b) were excluded because the standard deviations are considered when using ADNL, making the difference between the HVSRs for S-waves during strong and weak motions smaller. When the standard deviation is large as calculating the average HVSR, it seems to be more scientific and reasonable to use ADNL rather than DNL.

The proposed threshold of PNL was 7%, regarding a PGA threshold of 200 cm/s^2 . Beyond this value, 13 stations exhibited evident soil nonlinearity. Most of them were also identified based on DNL and ADNL thresholds, except for 51JZB, 51MXN, and 51TQL. Both DNL and ADNL represent an absolute change of amplitude from linear to nonlinear site response, but PNL represents a relative change percentage. The amplitudes of the linear

site response of stations 51JZB, 51MXN, and 51TQL are not large (Figs. 3, 4); in other words, the A_{\max} values are small, that is, 3.90, 3.53, and 7.86, respectively. This could inherently increase the relative change from linear to nonlinear site response. Therefore, in this case study, the performance of PNL is better than that of DNL and ADNL.

Based on RF_p , DNL, ADNL, and PNL, 11, 12, 10, and 13 stations, respectively, were identified as sites with evident soil nonlinearity during the Wenchuan main shock (Table 2). The results of this identification might vary based on different parameters because each parameter has an individual feature; however, to identify sites with very strong soil nonlinearity (e.g., 51WCW or 51SFB), any one of above four parameters would be effective. It is not easy to conclude whether the performance of RF_p is better or worse than that of DNL, ADNL, and PNL. For example, nonlinear site response was identified at station 51XJD using RF_p but cannot be identified based on DNL, ADNL, and PNL (Table 2). For station 62WUD, the identification is ineffective using RF_p but effective using DNL, ADNL, and PNL. This is because RF_p focuses on the shift of the predominant frequency, but the three other parameters focus on the change of amplitude from linear to nonlinear site response. Figure 10 shows that parameter f_{NL} is effective in evaluating the frequency band affected by soil nonlinearity, but less effective in identifying evidence of nonlinearity because this parameter cannot reflect the change of the predominant frequency or amplitude of the site response during weak and strong motions.

Table 2 Strong-motion stations with evident nonlinear site response during the Wenchuan main shock based on identification with RF_p , DNL, ADNL, and PNL, respectively

No.	Station code	Parameters used to identify the soil nonlinearity				Nonlinearity level
		RF_p	DNL	ADNL	PNL	
1	51AXT	●	●	●	○	Medium
2	51GYS	●	●	●	●	Strong
3	51GYZ	●	●	●	●	Strong
4	51JYC	●	●	●	●	Strong
5	51JYD	●	●	●	●	Strong
6	51JYH	●	●	●	●	Strong
7	51JZB	○	○	○	●	Medium
8	51JZW	●	●	○	●	Medium
9	51LXT	○	●	○	○	Medium
10	51MXN	○	○	○	●	Medium
11	51MZQ	●	●	●	●	Medium
12	51SFB	●	●	●	●	Strong
13	51TQL	○	○	○	●	medium
14	51WCW	●	●	●	●	Strong
15	51XJD	●	○	○	○	Medium
16	62WUD	○	●	●	●	Medium

● and ○ mean that the site response does and does not evidently behave nonlinearly

PNL, to characterize the nonlinear behavior of soil. The characteristics, performance, and effective usage of these parameters were analyzed, and their correlations with PGA, PGV, V_{S30} , and A_{max} were investigated. Based on this, the following conclusions were drawn:

- (1) RF_p , DNL, ADNL, and PNL all have strong positive correlations with PGA and PGV, whereas fNL has a negative correlation. The DNL also correlates well with A_{max} , but fNL shows no correlation with either A_{max} or V_{S30} . The empirical relationships between DNL and PGA and PGV, DNL and A_{max} , ADNL and PGA and PGV, ADNL and A_{max} , fNL and PGA and PGV, PNL and PGA and PGV, and PNL and A_{max} were all regressed, and moderate correlation coefficients were determined.
- (2) Overall, 16 sites were found to exhibit strong and medium soil nonlinearity during the main shock of the Wenchuan Earthquake, where the ground-motion level was almost beyond a threshold of $PGA > 200 \text{ cm/s}^2$ or $PGV > 15 \text{ cm/s}$; 14 sites exhibited weak nonlinearity; and 3 sites exhibited no nonlinearity. The thresholds of ADNL and PNL are proposed to be 2.0 and 7%, respectively, beyond which the site response represents evident nonlinear behavior. Eight sites (51MZQ, 51WCW, 51SFB, 51JYD, 51JYC, 51JYH, 51GYZ, and 51GYS) could be identified using any of the four parameters, RF_p , DNL, ADNL, and PNL, whereas the other eight sites (51AXT, 51JZW, 51XJD, 51LXT, 51MXN, 51TQL, 51JZB, and 62WUD) could be identified using individual parameters. This study confirms that RF_p , DNL, ADNL, and PNL all are effective in identifying the soil nonlinearity and can be selected based on user preference. The performance of PNL is better than that of DNL and ADNL in this case study.
- (3) The good correlations between DNL (ADNL, PNL) and PGA and PGV and between DNL (ADNL, PNL) and A_{max} imply that the degree of soil nonlinearity not only depends on the ground-motion amplitude (e.g., PGA or PGV) but also on the site condition. However, the frequency width affected by soil nonlinearity predominantly depends on the ground-motion level rather than the site condition, as inferred by the phenomenon that fNL has a good correlation with PGA but does not correlate with V_{S30} or A_{max} .

Abbreviations

A_{max} : maximum amplitude of HVSR calculated using weak motions; ADNL: absolute degree of nonlinearity; DNL: degree of nonlinearity; F_p : site-predominant frequency; fNL: frequency of nonlinearity; GIT: generalized inversion technique; HVSR: horizontal-to-vertical spectral ratio; KIK-net: Kiban Kyoshin

network; K-NET: Kyoshin network; NGA: next-generation attenuation; PGA: peak ground acceleration; PGV: peak ground velocity; PNL: percentage of nonlinearity; RF_p : ratio of predominant frequency; V_{S30} : average uppermost 30-m shear-wave velocity.

Authors' contributions

YFR analyzed the data, interpreted the results, and drafted the manuscript. RZW designed the study, interpreted the results, and made conclusions. XXY and KJ collected strong-motion records and processed the data. All authors read and approved the final manuscript.

Acknowledgements

The authors thank Kuo-liang Wen from the National Central University, Taiwan, for suggestions with respect to this study. We thank two anonymous reviewers for their valuable suggestions and constructive comments, which have considerably improved the quality of the manuscript.

Competing interests

The authors declare that they have no competing interests.

Data and resources

Strong-motion records used in this article were obtained from the China Strong-Motion Networks Center at <http://www.csmnc.net/> (last accessed December 2012). The V_{S30} measurements were taken from the Next Generation Attenuation (NGA) site database of the Pacific Earthquake Engineering Research (PEER) Center at <http://peer.berkeley.edu/ngawest2/databases/> (last accessed February 2015). Some of the figures were produced using Generic Mapping Tools (GMT).

Funding

This work was supported by the Science Foundation of the Institute of Engineering Mechanics, China Earthquake Administration (Grant No. 2016A04), National Natural Science Fund (No. U1534202), and Nonprofit Industry Research Project of the China Earthquake Administration (Grant No. 201508005).

Publisher's Note

Springer Nature remains neutral with regard to jurisdictional claims in published maps and institutional affiliations.

Received: 27 February 2017 Accepted: 8 August 2017

Published online: 22 August 2017

References

- Aguirre J, Irikura K (1997) Nonlinearity, liquefaction, and velocity variation of soft soil layers in Port Island, Kobe, during the Hyogo-ken Nanbu earthquake. *Bull Seismol Soc Am* 87:1244–1258
- Ancheta TD, Darragh RB, Stewart JP, Seyhan E, Silva WJ, Chiou BSJ, Wooddell KE, Graves RW, Kottke AR, Boore DB, Kishida T, Donahue JL (2013) PEER NGA-West2 database. PEER report, 2013/03
- Beresnev IA, Wen KL (1996) Nonlinear soil response—a reality. *Bull Seismol Soc Am* 86:1964–1978
- Beresnev IA, Field EH, Abeele KVD, Johnson PA (1998) Magnitude of nonlinear sediment response in Los Angeles basin during the 1994 Northridge, California, Earthquake. *Bull Seismol Soc Am* 88:1079–1084
- Bonilla LF, Tsuda K, Pulido N, Régner J, Laurendeau A (2011) Nonlinear site response evidence of K-NET and KIK-net records from the 2011 off the Pacific coast of Tohoku Earthquake. *Earth Planets Space* 63:785–789. doi:10.5047/eps.2011.06.012
- Boore DM (2010) TSPP-A collection of FORTRAN programs for processing and manipulating time series. U.S. Geol. Surv. Open-File Rept. 2008–1111, revision 2.11
- Borchardt RD, Glassmoyer G (1992) On the characteristics of local geology and their influence on ground motions generated by the Loma Prieta earthquake in the San Francisco Bay region, California. *Bull Seismol Soc Am* 82:603–641
- Celebi M, Prince J, Dietel C, Onate M, Chavez G (1987) The culprit in Mexico City-amplification of motions. *Earthq Spectra* 3:315–328

- Delépine N, Lenti L, Bonnet G, Semblat JF (2009) Nonlinear viscoelastic wave propagation: an extension of nearly constant attenuation (NCQ) models. *J Eng Mech* 135:1305–1314. doi:10.1061/(ASCE)0733-9399(2009)135:1(1305)
- Dhakal YP, Aoi S, Kunugi T, Suzuki W, Kimura T (2017) Assessment of nonlinear site response at ocean bottom seismograph sites based on S-wave horizontal-to-vertical spectral ratios: a study at the Sagami Bay area K-NET sites in Japan. *Earth Planets Space* 69:29. doi:10.1186/s40623-017-0615-5
- Dimitriu P (2002) The HVSR technique reveals pervasive nonlinear sediment response during the 1994 Northridge earthquake (M_w 6.7). *J Seismol* 6:247–255
- Field EH, Johnson PA, Beresnev IA, Zeng Y (1997) Nonlinear ground-motion amplification by sediments during the 1994 Northridge earthquake. *Nature* 390:599–602
- Hartzell S (1998) Variability in nonlinear sediment response during the 1994 Northridge, California, Earthquake. *Bull Seismol Soc Am* 88:1426–1437
- Li XJ (2009) Uncorrected acceleration records from fixed observation for Wenchuan Ms8.0 aftershocks. Seismological Publishing House, Beijing **(in Chinese)**
- Li XJ, Zhou ZH, Yu HY, Wen RZ, Lu DW, Huang M, Zhou YN, Cu JW (2008) Strong motion observations and recordings from the great Wenchuan earthquake. *Earthq Eng Eng Vib* 7:235–246
- Noguchi S, Sasatani T (2008) Quantification of degree of nonlinear site response. In: 14th world conference on earthquake engineering, Beijing, paper ID: 03-03-0049
- Noguchi S, Sasatani T (2011) Nonlinear soil response and its effects on strong ground motions during the 2003 Miyagi-Okii intraslab earthquake. *Zisin* 63:165–187 **(in Japanese with English abstract)**
- Pavlenko O, Irikura K (2002) Nonlinearity in the response of soils in the 1995 Kobe earthquake in vertical components of records. *Soil Dyn Earthq Eng* 22:967–975
- Pavlenko O, Loh CH (2005) Nonlinear identification of the soil response at Dahan downhole array site during the 1999 Chi-Chi earthquake. *Soil Dyn Earthq Eng* 25:241–250. doi:10.1016/j.soildyn.2004.08.004
- Pavlenko O, Wen KL (2008) Estimation of nonlinear soil behavior during the 1999 Chi-Chi, Taiwan, Earthquake. *Pure Appl Geophys* 165:373–407. doi:10.1007/s00024-008-0309-9
- Régnier J, Cadet H, Bonilla LF, Bertrand E, Semblat JF (2013) Assessing nonlinear behavior of soils in seismic site response: statistical analysis on KiK-net strong-motion data. *Bull Seismol Soc Am* 103:1750–1770. doi:10.1785/0120120240
- Régnier J, Cadet H, Bonilla LF, Bard PY (2016) Empirical quantification of the impact of nonlinear soil behavior on site response. *Bull Seismol Soc Am* 106:1710–1719. doi:10.1785/0120150199
- Ren YF, Wen RZ, Yamanaka H, Kashima T (2013) Site effects by generalized inversion technique using strong motion recordings of the 2008 Wenchuan earthquake. *Earthq Eng Eng Vib* 12:165–184. doi:10.1007/s11803-013-0160-6
- Rong MS, Wang ZM, Woolery EW, Lyu YJ, Li XJ, Li SY (2016) Nonlinear site response from the strong ground-motion recordings in western China. *Soil Dyn Earthq Eng* 82:99–110. doi:10.1016/j.soildyn.2015.12.001
- Trifunac MD, Todorovska MI (1996) Nonlinear soil response—1994 Northridge, California, Earthquake. *J Geotech Eng ASCE* 122:725–735
- Wen KL (1994) Non-linear soil response in ground motions. *Earthq Eng Struct Dyn* 23:599–608
- Wen KL, Beresnev IA, Yeh YT (1994) Nonlinear soil amplification inferred from downhole strong seismic motion data. *Geophys Res Lett* 21:2625–2628
- Wen KL, Huang JY, Chen CT, Cheng YW (2011) Nonlinear site response of the 2010 Darfield, New Zealand earthquake sequence. In: 4th IASPEI/IAEE international symposium, 23–26 Aug 2011, Santa Barbara
- Xu XR (2010) Recognition soil nonlinearity area applying the time-frequency analysis method in Wenchuan earthquake. Dissertation, National Central University, Taiwan

Submit your manuscript to a SpringerOpen® journal and benefit from:

- Convenient online submission
- Rigorous peer review
- Open access: articles freely available online
- High visibility within the field
- Retaining the copyright to your article

Submit your next manuscript at ► springeropen.com
